MATERIALS ADAPTATION
for
DEVELOPING NATIONS

PROGRESS EVALUATION

by

Curtis Scott Smith
Jan T. Taniguchi

FERROCEMENT JOURNAL BEARING

by

Athar P. Ahmad

Advisor: Prof. Nathan H. Cook

May 1973

TABLE OF CONTENTS

		Page
I.	INTRODUCTION	1
II.	ANALYSIS OF FERRO-CEMENT PROPERTIES	3
	A. Optimum Mortar Strength Characteristics	3
	B. Qualitative Mesh Analysis Test	4
	C. Ultimate Bending Moment Test	4
	D. Deflection Due to Bending Moment Test (In the Uncracked Region)	5
III	CONCLUSIONS	7
	APPENDIX A	13
IV.	FERRO-CEMENT APPLICATION IN BEARINGS	1
	A. Cement Bearings without Reinforcement	1
	B. Discussion	4
	APPENDIX A	9

MATERIALS ADAPTATION FOR UNDERDEVELOPED COUNTRIES

I. INTRODUCTION

The long range goal of our experiment is to utilize ferro-cement as a substitute material for metal machine parts. To date, our experimentation has provided us with some properties of ferro-cement. When we speak of ferro-cement, we are referring to the composite mixture of portland cement mortar, pozzolan and sand, in combination with finely divided, closely spaced mesh. By no means do we consider our experimentation complete; however, at this point we wish to display and evaluate our data, in order to organize further experimentation. Through our experiments we hope to broaden the range of cement application by altering certain of its properties to fit a given situation. In other words, we hope to remove the present restrictions of cement use, dictated by its properties.

Our first consideration was the fact that cement had a high compressive strength (4,131 psi), while it has a tensile strength of only 400 psi.[1] We wish to employ steel to find the optimum combination with cement to form a new product with the properties of the hardness and cheapness of concrete, and the ductility and tensile strength provided by steel. Our first experiments were performed on unreenforced mortar, to find the optimum combination of ingredients. We then proceeded to determine the best mesh and its properties.

In the beginning our general approach was to find the qualitative, rather than the quantitative, properties. As we proceeded, we

---

1. Hans Frederick Muhlert, Analysis of Ferro-cement in Bending, pp. 1, 17.

began to gather more quantitative data, that could be used in applying ferro-cement to a typical machine part.

I has come to our attention that even though scientific methods demand measurements in the metric system, that most of the previous work that has been done in this field, has been done in the English system. Therefore, for ease in comparison, we will present our data in both systems.

II. ANALYSIS OF FERRO-CEMENT PROPERTIES

A. Optimum Mortar Strength Characteristics

Our procedure here was to make individual specimens (2.75" x 2.75" x 0.5"; 6.985 cm x 6.985 cm x 1.27 cm) and to test various proportions of water, sand, and cement. The particular ranges we tested were one part cement, 1.5-2.5 parts sand, .45-.55 parts water. (Proportions determined by weight). The apparatus for testing was a lathe dynamometer in which we fastened the specimen as shown in Figure 1.

We supplied the pressure by means of a 3/8" stainless steel ball bearing. At known pressure intervals, we released the specimen and measured the diameter of the indentation under an analytical microscope (Nikon Measurescope). We then utilized this data to determine the Brinell hardness, which was the trait we wished to maximize. Also maximum pressure before failure was recorded. Another property we determined was the average specific gravity of the mortar.

Two things are to noted here: 1) The indentations, to our surprise worked quite well, i.e. clear indentations were made without fracture or crumbling of the cement; 2) Upon reaching a given load, the pressure that the mortar exerted upon the dynamometer receded slightly with time.

Quite accidentally, we discovered a process by which a better cement bearing could be made. Our molds were made of a waxed cardboard, and we discovered that the cement had an incredibly smooth face when cast in this type of mold.

The mortar strength data is summarized and listed in Tables I and II.

B. Qualitative Mesh Analysis Test

The apparatus we devised for this test consisted of, once again, the lathe dynamometer, except that this time instead of a flat plate to mount our specimens, we utilized a V-notched piece of stock such that we could apply a load onto our specimens and they would bend inward until fracture. See Figure 2.

The only criterion we used for this experiment was maximum applied load prior to failure. The raw data can be found in the appendix, but the general conclusion we arrived at was that the meshes that provided the most promise were 1/2" weld, 1/4" woven, and 1/8" weld. (1.27 cm weld, .635 cm woven, .318 cm weld). Here it must be stated that we assumed catastrophic failure to mean an inadequately low mesh to mortar ratio. To begin with, our specimens were 2.75" x 2.75" x 0.5" (6.985 cm x 6.985 cm x 1.27 cm) and incorporated three layers of evenly spaced mesh each. It was determined by means of the previous assumption, that four layers of mesh were optimum in 1/8" weld. We therefore utilized this data in organizing our further experimentation. The specific data is listed in Table III.

C. Ultimate Bending Moment Test

In this test, our specimens wer 30 cm x 6 cm x 2 cm (11.8" x 2.35" x .785"). Specimens were grouped into five categories: 1) 1/2" weld; 2) 1/8" weld; 3) 1/4" woven (all having three evenly spaced layers); 4) 1/8" weld (four layers); 5) 1/8"-1/2"-1/8" weld. The specimens were tested on the universal testing machine. In order to come as close as possible to a perfect line load (theoretically, the pressure is not applied over an area, but in a perfect line), which in

reality can never be achieved, we used solid cylindrical bars as supports and also as a means of application of loads. The supports were placed at a distance of 20 cm from each other, while the load was applied symmetrically at a distance of 10 cm apart. This configuration results in a constant bending moment between the applied loads. (See Figure 3). Our data confirmed our hypothesis that an extra layer of mesh in the 1/8" specimen would strengthen it. In applying the load, the universal testing machine was set at a constant speed and let it advance until failure. As expected, fracture occurred axially along the layers of mesh and laterally along intersections in the mesh squares. Specific data is listed in Table IV.

D. Deflection Due to Bending Moment Test (In the Uncracked Region)

The specimens were used here were 5.75 x 2.75 x 0.75 (14.7 cm x 7.1 cm x 1.95 cm). We felt the need for a greater uniformity in our specimens, therefore, we purchased a set of clear plastic forms in which we measured off and marked equal spacing for mesh on the corners. We then filled the forms with cement up to each mark, vibrating with an offset motor attached to a platform, and at this point inserted a layer of mesh. This procedure was continued until the forms were filled, resulting in uniformity with a high degree of accuracy. Specimens were tested using a milling machine with a milling dynamometer, instead of the universal testing machine, so that we could accurately stop at known deflections and record the applied load. We also found that a stable and uniform support and loading system had to be machined to minimize deviations between individual tests.

As a sidelight to this experiment it was noticed that an extremely smooth specimen was produced simply by using the vibration technique in a plastic mold. We have not yet had time to utilize this in our bearing test.

The detailed forced deflection data is shown in Table V, while the bending moment deflection data is in Table VI, and is plotted in Figure 7.

III.

The optimum combination for the mortar mixture was 1 part cement, 2.5 parts sand, .45 parts water.

The best mesh ratio and configuration was found to be four layers per inch of 1/2" square weld, .063" diameter mesh. It was also noted that results comparable to that of the 1/2" mesh could be obtained by six layers per inch of 1/8" weld mesh, or five layers per inch of 1/4" woven mesh. We found the average specific gravity of our mexture (unreinforced) to be approximately 2.5 gm/cm^3.

In the bending moment tests, we obtained graphs that were roughly parabolic. We hypothesize from the following analysis that the strongest material will be the one that gives the closest approximation to a linear bending moment versus deflection diagram.

We know that for linear elastic deflections, the radius of curvature of the deflection of the specimen, ρ is inversely proportional to the bending moment, given by the following formula: $\rho = EI/M$; where E is the Young's modulus of the material; I the moment of inertia of the material configuration; and M the bending moment. For uniform specimens and loading conditions, the product EI is a constant. It can be therefore concluded that the overall best combination is 1/2" square mesh at four layers per inch. Even though the others were very close in fracture strength, plotting bending moment versus deflection (See Figure 7), it can be seen that the 1/2" weld yielded the most favorable results.

We also wish to explain some of our results by the hypothesis that the ferro-cement incorporates plastic, elastic, and time dependent

deformations. We base the hypothesis upon the fact that in the deflection due to bending tests (in the uncracked region), the material clearly behaved elastically. Plastic deformation is noted in the ultimate bending moment tests and the time dependent deformation is seen in our optimum mortar strength characteristics tests. As pointed out earlier, when a specified load was reached, the pressure that the mortar exerted upon the dynamometer receded slightly with time. Comparing the graphs made on the Sanborn 321 of the fracture tests on the reinforced and unreinforced concrete was quite interesting. It was noted that at the point of fracture, the pressure exerted by the unreinforced concrete dropped sharply, whereas, when the reinforced concrete fractured, the pressure asympototically approached a constant. This behavior we feel can be attributed to total failure in the concrete and the wire mesh accepting the total load at a given pressure point until failure. (See Figure 5).

We believe the greatest obstacle to overcome is to obtain good bonding between the wire mesh reinforcement and concrete. This incorporates many aspects: 1) to get the proper area to volume ratio per cubic inch of mesh, 2) by adjusting layers of mesh per inch, 3) to determine the best chemical properties for bonding. We felt it necessary to obtain better bonding; for in our experiments at fracture the concrete separated from the mesh into small cubes, between layers within squares. Also most fracture occurred along the lines of mesh. (See Figure 6).

Finally, taking our data in total, we find that with four layers of 1/2" mesh in a 3/4" thick slab, we could achieve the following

properties:

Maximum loading stress before cracking	1500 psi.
Maximum loading stress at gross deformation	2000 psi.
Equivalent modulus of elasticity	3×10^6 psi.

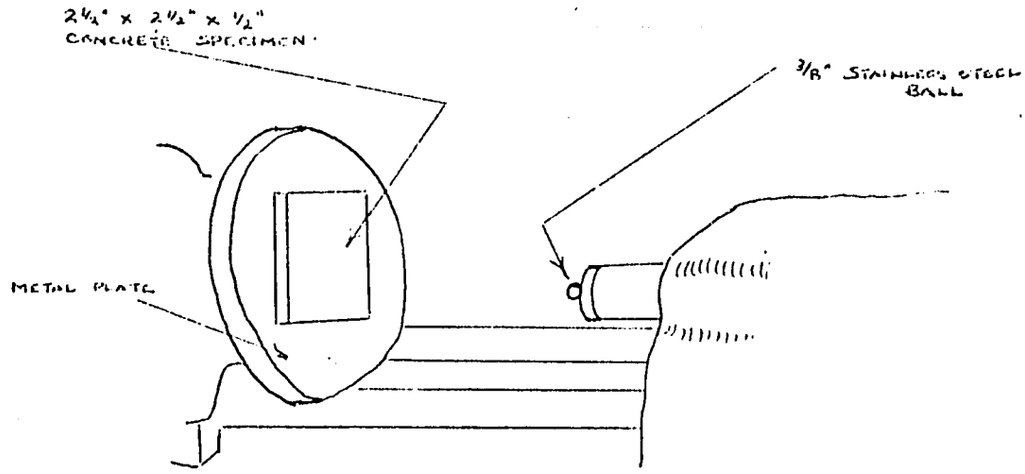

Figure 1. This is the apparatus used in the Optimum Mortar Strength Characteristics test. The shaft to which the 3/8" stainless steel ball is fixed advances perpendicular to the plane of the specimen. All other parts of the apparatus were fixed.

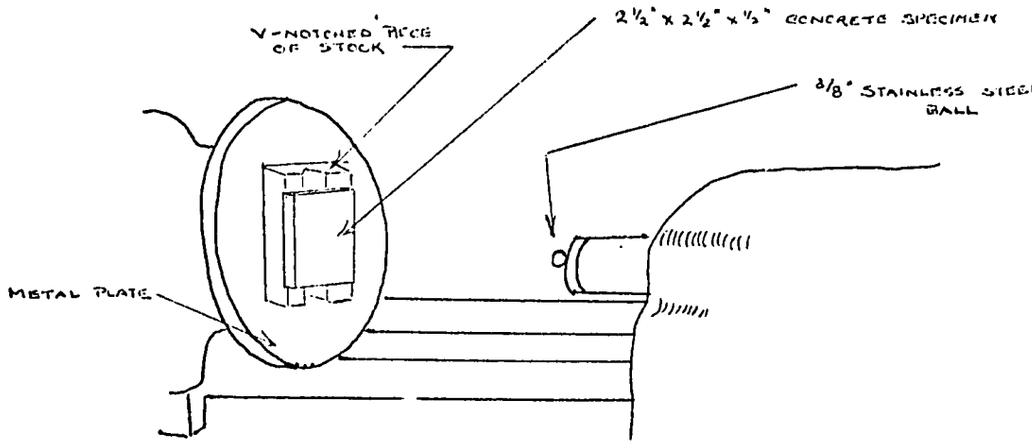

Figure 2. This is the apparatus for the Qualitative Mesh Analysis Test. It is similar to that of Figure 1, except for the introduction of the V-notched piece of stock to permit bending to fracture.

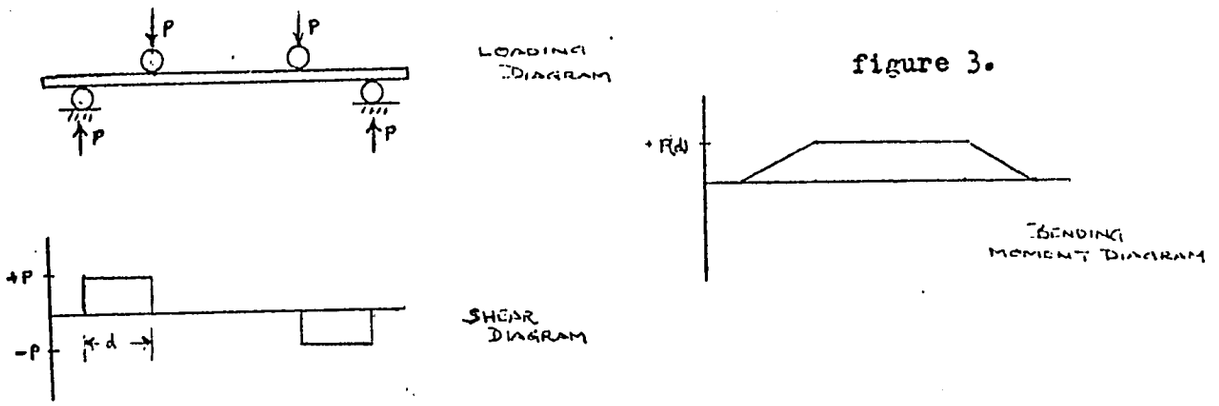

figure 3.

The portion of the figure in the upper left shows the configuration of the testing apparatus for the Ultimate Bending Moment Test. The diagrams in the lower left and right show the shear and bending moment distributions, respectively, as you travel from left to right in the specimen.

figure 4.

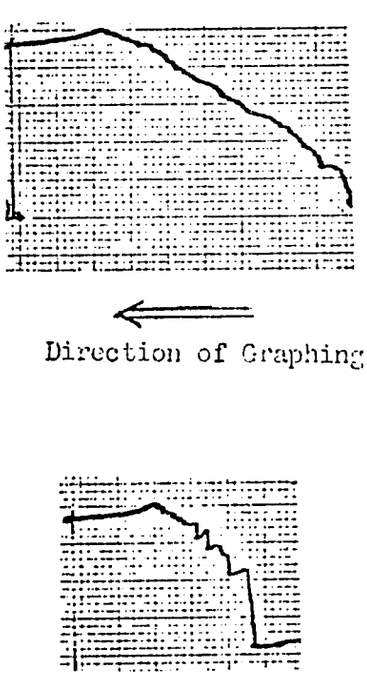

Direction of Graphing

Graph speed, 1mm/sec. This figure shows examples of time dependant deformation. As can be seen, after maximum load is reached, pressure falls off with time.

figure 5.

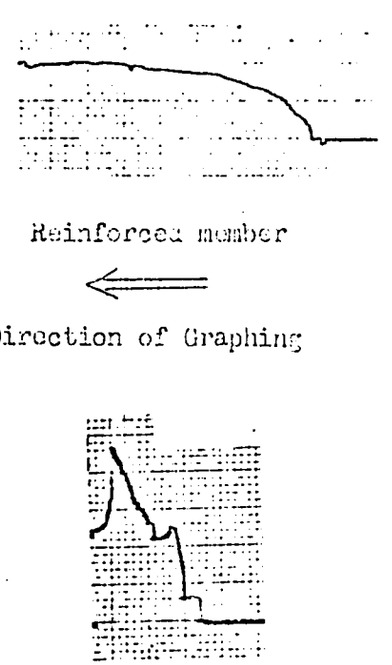

Reinforced member

Direction of Graphing

Unreinforced member

Graph speed, 1mm/sec. This figure shows the difference in failure between the reinforced and unreinforced members.

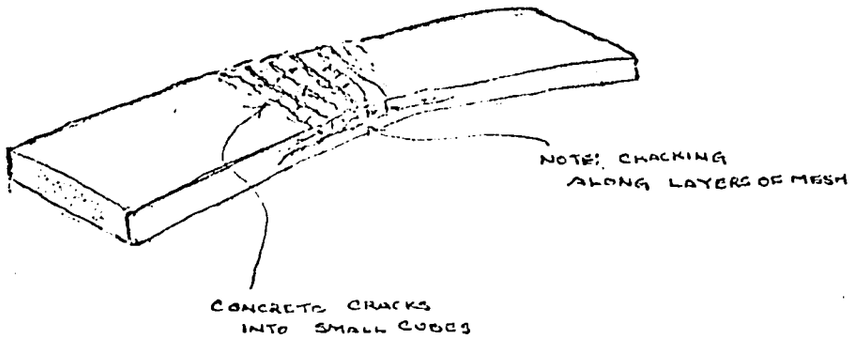

Figure 6 This diagram illustrates the typical fracture mechanism in ferro-cement.

APPENDIX A

TABLE I

OVERVIEW OF THE DATA FOR THE OPTIMUM MORTAR STRENGTH CHARACTERISTICS

Explanation of Nomenclature:

Series I; Sand-Cement Ratio of 1.5
Series II; Sand-Cement Ratio of 2.0
Series III; Sand-Cement Ratio of 2.5

Series A; Water-Cement Ratio of .45
Series B; Water-Cement Ratio of .50
Series C; Water-Cement Ratio of .55

Two specimens made for each combination of series Numbers and Letters

Average Hardness for Series Groupings;
s-sand, c-cement, w-water

Series	Average Hardness (kg/mm^2)
I (s/c=1.5)	110
II (s/c=2.0)	83
III (s/c=2.5)	135
A (w/c=.45)	139
B (w/c=.50)	102
C (w/c=.55)	87

The specific data can be found in Table II.

TABLE II

TABLE OF DATA FOR THE OPTIMUM MORTAR STRENGTH CHARACTERISTICS TEST

Specimen	Load lbs.	Indentation Diameter 1/1000"	Brinell Hardness kg/mm^2
I-A1	200	88.65	110
"	250	97.6	113
"	300	121.4	87
"	350	126.3	93
"	400	100.05	173
"	600	103.9	238
"	760	---	Fracture
I-A2	200	73.9	159
"	250	94.15	122
"	270	---	Fracture
I-B1	200	106.6	75
"	250	114.3	82
"	300	109.4	108
"	340	---	Fracture
I-B2	200	77.6	145
"	250	82.3	161
"	300	94.6	145
"	350	107.3	131
"	400	112.5	130
"	600	116.35	189
"	800	---	Fracture
I-C1	200	97.2	91
"	250	118.35	76
"	300	140.8	52
"	500	---	Fracture
I-C2	200	81.85	129
"	250	120.05	74
"	300	136.5	68
"	350	145.15	70
"	400	---	Fracture
II-A1	200	106.7	75
"	250	100.1	108
"	300	137.81	68
"	350	121.1	102
"	400	118.55	122
"	620	---	Fracture

TABLE II

(Continued)

Specimen	Load lbs.	Indentation Diameter 1/1000"	Brinell Hardness kg/mm^2
II-A2	200	90.8	105
"	250	109.4	90
"	300	111.2	93
"	350	129.0	90
"	400	134.5	93
"	570	---	Fracture
II-B1	200	97.15	92
"	250	109.05	90
"	300	128.2	78
"	295	---	Fracture
II-B2	200	119.6	60
"	250	129.65	63
"	300	140.05	65
"	340	---	Fracture
II-C1	200	106.4	76
"	250	106.6	94
"	300	115.8	96
"	350	---	Fracture
II-C2	200	113.45	67
"	250	127.7	66
"	300	132.7	73
"	350	---	Fracture
III-A1	200	50.35	342
"	250	75.55	192
"	300	81.05	199
"	350	97.25	162
"	400	90.85	209
"	600	126.15	161
"	660	---	Fracture
III-A2	200	64.15	212
"	250	72.15	210
"	300	70.85	162
"	350	103.1	142
"	400	100.65	169
"	600	120.45	177
"	710	---	Fracture

TABLE II

(Continued)

Specimen	Load lbs.	Indentation Diameter 1/1000"	Brinell Hardness kg/mm^2
III-B1	200	100.45	86
"	250	108.85	90
"	300	110.75	105
"	350	129.1	89
"	400	120.6	118
"	600	143.15	124
"	670	---	Fracture
III-B2	200	92.45	101
"	250	103.85	99
"	300	122.95	84
"	350	124.0	97
"	400	131.65	98
"	320	---	Fracture
III-C1	200	103.5	80
"	250	132.0	61
"	270	---	Fracture
III-C2	200	72.1	146
"	250	91.5	129
"	285	---	Fracture

TABLE III

DATA FOR THE QUALITATIVE MESH ANALYSIS TEST

Two specimens each for five series were made. These series are as follows:

Series 1 - 1/2" weld,	wire size .060*	area/volume =	63.7
Series 2 - 1/4" weld,	wire size .025	area/volume =	160.0
Series 3 - 1/4" woven,	wire size .041	area/volume =	97.5
Series 4 - 1/3" weld,	wire size .032	area/volume =	125.0
Series 5 - 1/8" weld,	wire size .017	area/volume =	235.0

* metric equivalents can be found in main body.

Series	Pressure at Fracture
1A	1,125
1B	1,000
2A	650
2B	550
3A	600
3B	700
4A	500
4B	650
5A	650
5B	950

TABLE IV

DATA FOR THE ULTIMATE BENDING MOMENT TEST

Four specimens each for five series were made. These are as follows:

Series A - 1/2" weld, 4 layers/inch

Series B - 1/4" woven, 4 layers/inch

Series C - 1/8" weld, 4 layers/inch

Series D - 1/8" weld, 6 layers/inch

Series E - 1/2" weld, 1/8" weld, 1/2" weld

Series	Ultimate Recorded Pressure
A1	410
A2	600
A3	420
A4	550
B1	150
B2	205
B3	230
B4	242
C1	500
C2	400
C3	470
C4	460
D1	494
D2	540
D3	420
D4	525
E1	430
E2	338
E3	400
E4	250

TABLE V

DATA AND RESULTS FOR THE DEFLECTION DUE TO BENDING MOMENT TEST (IN THE UNCRACKED REGION)

Five specimens each for three series. These series are as follows:

Series A - 1/2" @ 4 layers/inch

Series B - 1/4" @ 5 layers/inch

Series C - 1/8" @ 6 layers/inch

Series	Pressure at .01" Deflection	at .02"	at .03"	at .04"	at .05"	at .06"	at .07"	at .08"	at .09"
A1	160	350	500	750	900	1,150	1,350	---	---
A2	50	200	320	500	725	850	1,120	1,300	1,500
A3	150	250	500	750	780	1,050	1,300	1,500	---
A4	75	175	320	450	625	850	1,100	1,400	---
A5	100	220	300	475	650	825	1,000	1,250	1,550
B1	75	170	250	425	670	900	1,160	1,400	---
B2	55	130	200	330	425	670	850	1,150	1,400
B3	20	85	175	270	375	600	750	1,000	1,250
B4	85	200	325	500	750	900	1,250	1,450	---
B5	55	150	260	375	625	875	1,050	1,350	---
C1	65	160	250	380	525	725	855	1,100	1,300
C2	75	200	275	450	600	880	975	1,250	1,360
C3	25	80	150	235	370	500	720	800	1,050
C4	75	230	300	600	825	950	1,200	---	---
C5	60	170	270	375	500	650	750	950	1,150

TABLE VI

DEFLECTION DUE TO BENDING MOMENT TEST CONTINUED

	M_b (ft-lbs)							
Specimen	at .01"	at .02"	at .03"	at .04"	at .05"	at .06"	at .07"	at .08"
A1	2.62	5.74	8.20	12.30	14.76	18.87	22.15	---
A2	.82	3.28	5.25	8.20	11.89	13.94	18.37	21.33
A3	2.46	4.10	8.20	12.30	12.80	17.23	21.33	24.61
A4	1.23	2.87	5.25	7.38	10.25	13.94	18.05	22.97
A5	1.64	3.61	4.92	7.79	10.66	13.53	16.41	20.51
B1	1.23	2.79	4.10	6.97	10.99	14.76	19.03	22.97
B2	.90	2.13	3.28	5.41	6.97	10.66	13.94	18.87
B3	.33	1.39	2.87	4.43	6.15	9.84	12.30	16.40
B4	1.39	3.28	5.33	8.20	12.30	14.76	20.51	23.79
B5	.90	2.46	4.27	6.15	10.25	14.35	17.23	22.15
C1	1.07	2.62	4.10	6.23	8.61	11.89	14.03	18.05
C2	1.23	3.28	4.51	7.38	9.84	14.44	15.99	20.51
C3	.41	1.31	2.46	3.86	6.07	8.20	11.81	13.12
C4	1.23	3.77	4.92	9.84	13.53	15.58	19.69	---
C5	.98	2.79	4.43	6.15	8.20	10.66	12.30	15.58

Figure 7a

Graph of deflection versus bending moment for the Deflection Due to Bending Moment Test

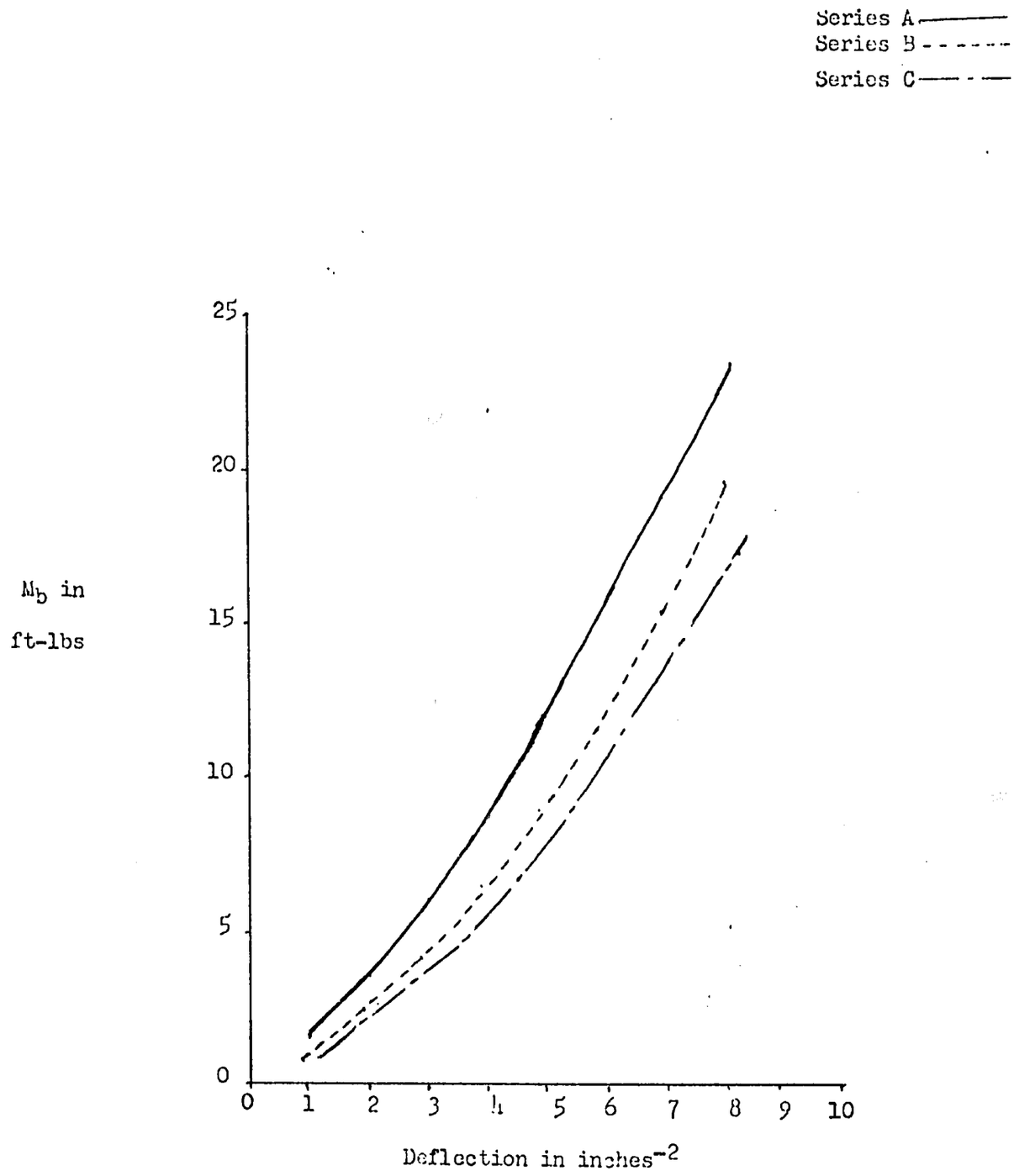

Figure 7b

Graph of deflecton versus bending moment for the Deflection Due to Bending Moment Test

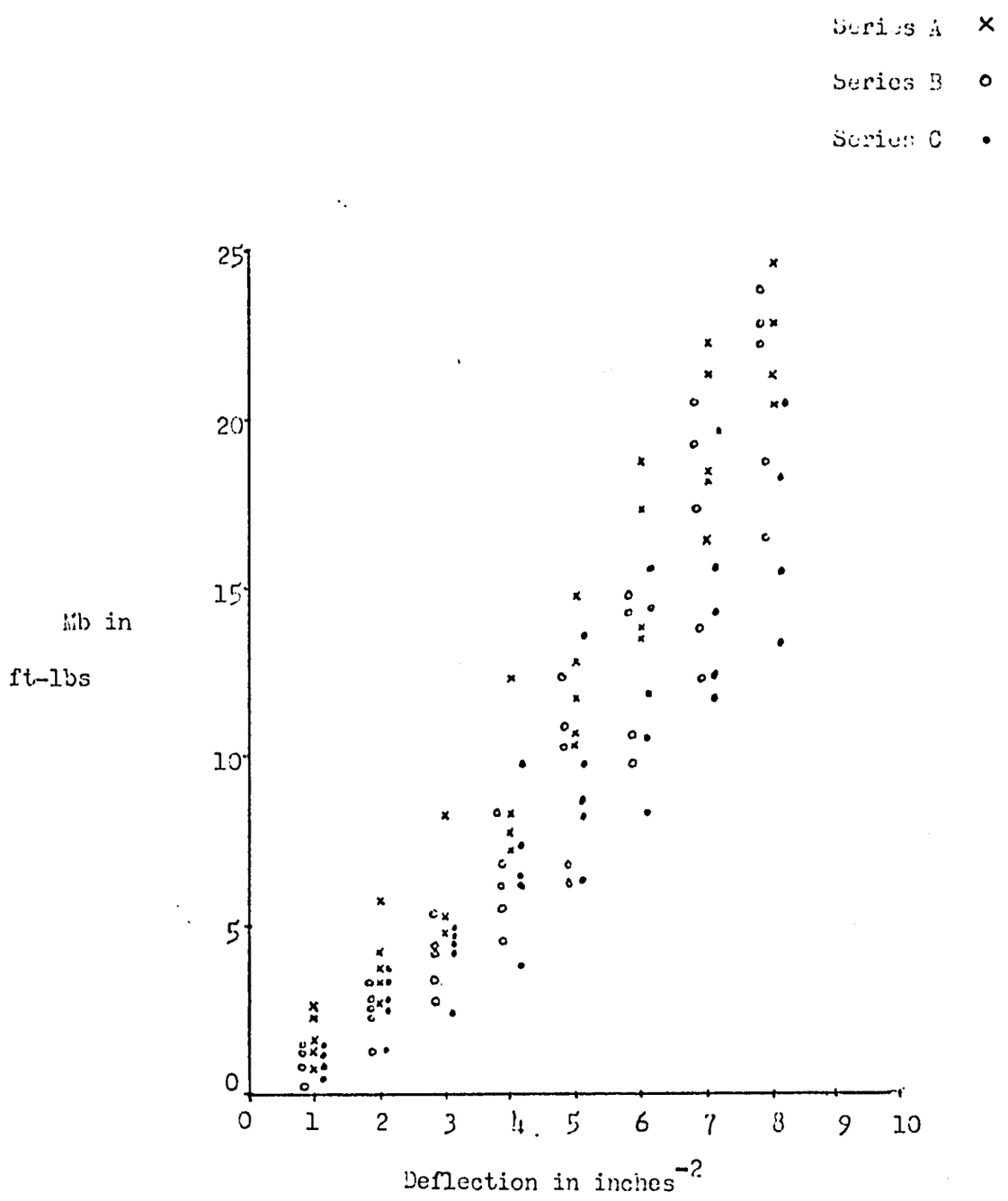

TABLE VII

MATERIALS

Cement: Type III Portland Cement

Aggregate: Huber Professional Grower's Top Soil (Pozzolan and Sand)

Wire Mesh:

Mesh Size	Comments	Wire Diameter	Area/Vol.
1/2" sq.	weld	.063"	63.7
1/4" sq.	weld	.025"	160.0
1/4" sq.	woven	.041"	97.5
1/3" sq.	weld	.032"	125.0
1/8" sq.	weld	.017"	235.0

FERRO-CEMENT APPLICATION IN BEARINGS

A. Cement Bearings without Reinforcement

A mixed solution of sand and cement in water in the ratio, (1:1:1/2::sand:cement:water) by weight was poured in aluminum molds with a steel rod glued to the surface and situated in the center of the mold (aluminum cylinder). Mixing and pouring of the concrete was done on a mixing table to obtain maximum homogeneity of the concrete and insure good setting of concrete in the molds. The rods were coated with wax to a thickness of 3/1000 - 5/1000" to provide the separation between the bearing surface and the rotating rod.

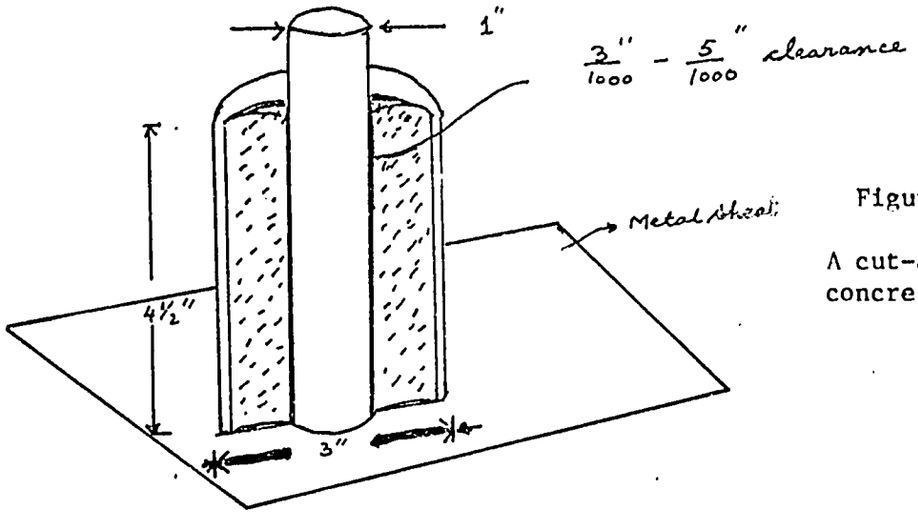

Figure 1.

A cut-away of the concrete bearing.

Ten samples of cement bearings have been made so far. All of these are without any reinforcements. Six out of these ten were examined and a series of tests were run on these to determine the bearing characteristics. Two of these samples (#1 and #2) were run without any lubricant while the other four were lubricated with oil. The data obtained is given in Table 1 through Table 6.

Samples #3-#6 were lubricated by boring a hole through the bearing surface and continuously pouring oil through the hole as the carbide steel journal rotated inside the bearing. The separation between the journal and the bearing was between 3/1000" and 5/1000". Thus the average thickness of the oil film would be around 3/1000" to 5/1000".

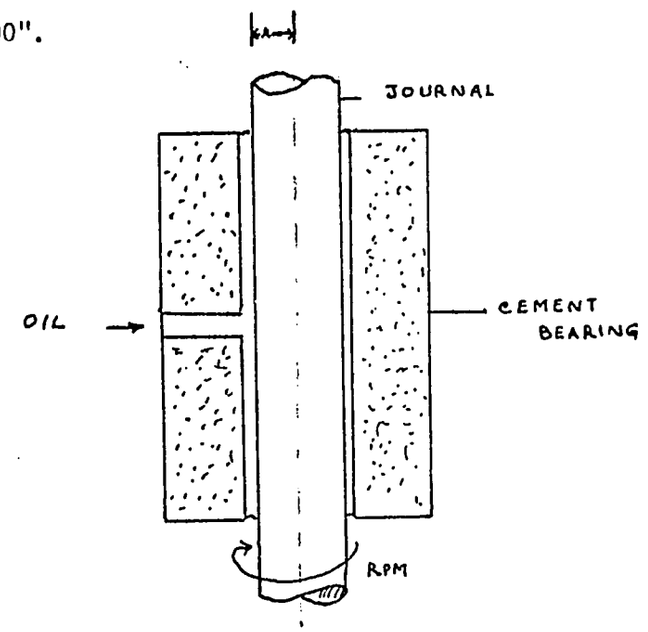

Figure 2

The measurements given in Table 1 through Table 6 were obtained in the following manner. The sample (cement bearing) together with the journal (carbide steel rod, polished on a lathe to a diameter of 1") was set on the dynamometer. (See Figure 3).

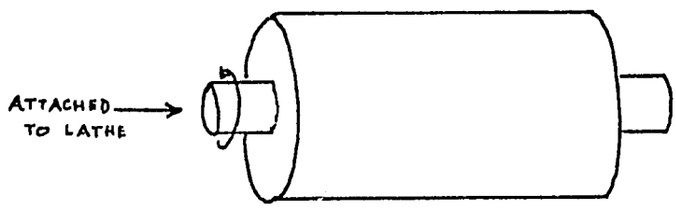

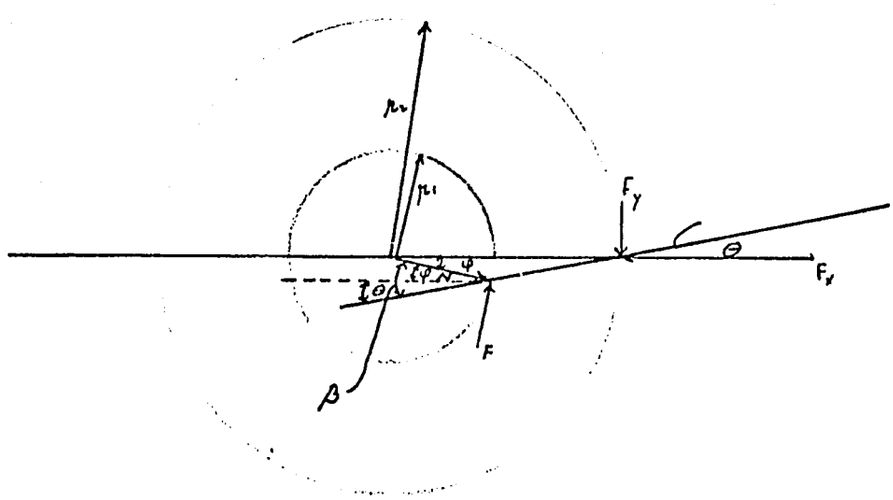

FOR SMALL ANGLES θ, φ

$$\tan\theta = \frac{F_y}{F_x} = \theta,$$

$$r' = r_2 - r_1, \quad \tan\varphi = \frac{r'\theta}{r_1}$$

$$\beta = \theta + \varphi$$

$$\tan\beta = \frac{F}{N} = \mu = \text{coefficient of friction}$$

$\therefore$ coefficient of friction

$$\mu = \tan\beta = \tan(\theta + \varphi)$$

$$= \tan\left[\tan^{-}\frac{F_y}{F_x} + \tan^{-}\left[\left(\frac{r_2 - r_1}{r_1}\right)\frac{F_y}{F_x}\right]\right]$$

FIG. 3

The applied load on the bearing is denoted by F_x. It was applied at the center of the bearing. The vertical force F_y was measured. F_x was varied for different revolutions per minute of the journal and F_y was measured. Both F_x and F_y were simultaneously plotted on the graph paper. For the samples with lubrication, oil was poured through the hole as the journal rotated inside the bearing.

B. Discussion

Table 1 and 2 give the bearing load, frictional force, and the coefficient of friction for samples #1 and #2, which were run without any lubricant. The coefficient of friction is fairly constant for these two samples. However, the maximum RPM's that could be obtained without immediate heating-up and cracking of the cement surface was 275 RPM accompanying a load of 250 lbs. This was the upper limit for maximizing RPM's and bearing load. At this point, (and at various other points, see Table 1 and 2) concrete chips began to fall off and the bearing heated up. No temperature curve was made for this sample or any others. No efficient method had been devised by the author at the time of experimentation to simultaneously record the temperature at the surface of the bearing and the journal as the load and RPM's were varied.

Alignment problems were encountered as the journal was not exactly centered due to difficulties in the molding techniques. As a result of this, the graph that showed the variation in F_x and F_y was only approximate. Instead of a constant value for F_x and F_y, we got a sinusoidal variation, the frequency of which corresponded to the

frequency with which the journal was rotating. Thus an average for both F_x and F_y was established from the graph.

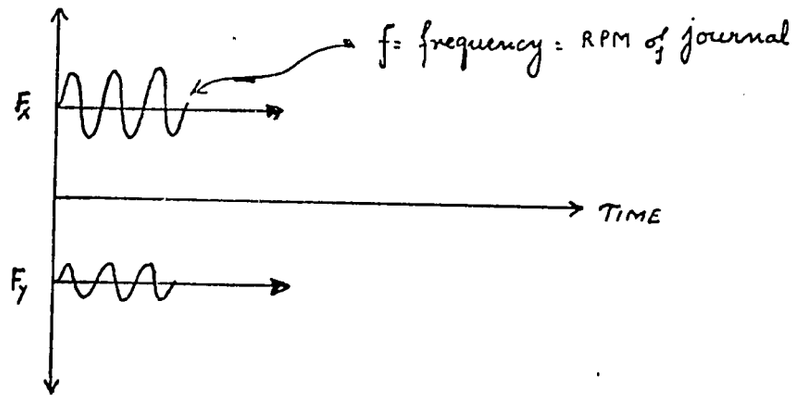

Graph 1

A test was done to determine the bearing life. After two hours of running at a load of 200 lbs. and at 200 RPM the bearing started chipping off and cracked. Figure 4 shows a microscopic photograph (magnification 50X) of the cracks that had appeared in the bearing after a run of one and a half hours. A cement bearing with no lubrication and carbide steel journal seems to have little practical value because of unusually short life, low loading capacity, and relatively high coefficient of friction.

Figure 4

Tables 3 through 6 give the data obtained from cement bearings that were lubricated by lubrication oil. Again, the coefficient of friction is fairly constant for loads up to 500 lbs. and 1000 RPM. This combination 500 lbs (bearing load) and 1000 RPM was the maximum, the bearing could hold. At that point, oil started burning and the bearing heated to such an extent that concrete fell off. However, due to lack of an efficient method, no temperature curve was drawn in this case. Samples #3-#6 were of high quality compared to samples #1 and #2 with respect to their surface characteristic. The wax coating had produced an unusually smooth concrete surface on which the journal rotated.

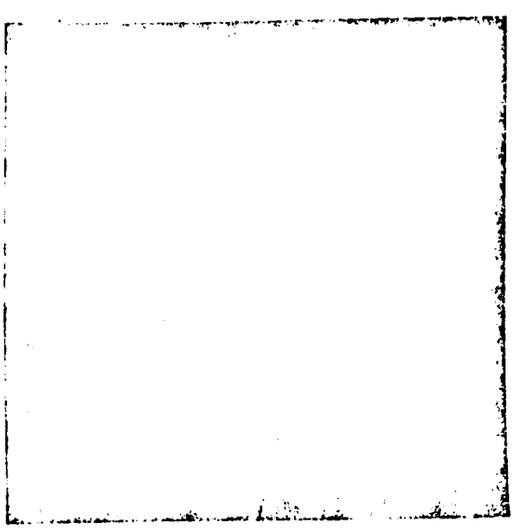

Figure 5

Sample #3 was run for two hours at 500 RPM and 250 lbs. load. A photomicrograph of the sample is shown in Figure 5. As with previous samples, cracks appeared in this sample too. However, there is an uncertainty about the crack in Figure 5. Since a piece of the bearing

surface was used to take a photomicrograph, the crack might have appeared while cutting the piece. There was no obvious cracks on the outer surface as was the case for samples #1 and #2.

There are several factors that must be considered when one compares the performance of the bearing. Compatibility is a measure of the anti-weld characteristic of a bearing material when operated with a given journal material. Metal to metal contact exists frequently even in well lubricated journal bearings. Upon starting, the rotating journal slides on the bearing until an oil film is generated to separate the surfaces. Embeddability and Conformity: The hardness and modulus of elasticity of a bearing material should be as low as possible while providing sufficient strength to carry applied loads. The resulting characteristics enable a bearing to compensate for misalignment and to conform to geometric errors. Compressive and Fatigue strength: Fatigue strength is particularly important in applications for which load changes direction, such as reciprocating engines. A sufficiently high fatigue strength will enable a bearing to operate without developing cracks or surface chips. Tables 1 through 6 give data showing these characteristics for materials used for journal bearing and similar tests performed as those performed with cement by E. H. Scott, Jr., and E. R. Booster (published in "Product Engineering," September 1952). If we compare the coefficient of friction of the cement journal bearings for both the dry samples and those with oil, the cement bearings look very good. However, in view of the fact that despite many methods (I was unable to get smooth surfaces) and the geometrical errors made in setting up the mold, such "good" results on friction are questionable.

It was difficult to make an exact "clearance" between the journal and the bearing (the optimum is supposedly 3/1000"). Therefore, this area is subject to error. (Other samples are ready to try this again, both dry and with oil). Note: In the samples tested by Scott and Booster, as shown in Table 2, one drop of oil was used. In our samples, oil was continuously poured.

The areas where my samples fare very poorly are in wear-rate and load capacity. Looking back at our data, the maximum load obtained so far with 500 RPM was 70 psi. As shown in Table 1 and Table 2, this is much lower than any of the materials Booster and Scott had used. Although no curve was drawn in the case of the cement bearings to show the wear rate, the wear rate in my samples was very high. As already discussed, in some samples, after two hours of running, the bearing had cracked and concrete chips had fallen off, increasing the "clearance" and immediately causing ever increasing wobbling.

Reinforced bearings are in the process of being tested.

APPENDIX A

COMPLETE SETS OF DATA AND COMPARATIVE RESULTS FOR THE BEARING TESTS

	RPM's	F_x (lbs)	F_x/A (psi)	F_y (lbs)	μ
Sample 1	150	55	9.2	12	.73
(no lubricant)	150	120	20	22	.53
	150	200	33.4	50	.87
	250	160	27.7	40	.87
Sample 2	125	60	8.6	13	.70
(no lubricant)	175	100	14.3	25	.81
	200	150	21.2	39	.90
	250	75	10.7	16	.70
	275	150	21.2	33	.75
Sample 3	110	50	7.15	4	.24
(oiled)	110	110	15.7	9	.24
	110	160	22.9	11	.21
	110	200	28.6	18	.27
	1000	120	17.2	8	.21
	1000	250	35.7	22	.27
	1000	500	71.5	-	-
Sample 4	200	60	8.6	5	.24
(oiled)	200	120	17.2	10	.24
	200	180	25.7	16	.27
	200	220	31.4	20	.27
	200	250	35.7	23	.27
	250	250	35.7	25	.32
Sample 5	300	60	8.6	5	.24
(oiled)	300	140	20	13	.27
	300	200	28.6	20	.32
	300	250	35.7	23	.27
	300	500	71.5	60	.36
	350	200	28.6	18	.27
	350	250	35.7	23	.27
	350	500	71.5	55	.34
Sample 6	400	60	8.6	5	.24
(oiled)	400	100	14.3	9	.27
	400	150	21.2	14	.27
	400	250	35.7	25	.32
	500	100	14.3	9	.27
	500	150	21.2	12	.24
	500	200	28.6	20	.32
	500	250	35.7	22	.27
	500	500	71.5	50	.32

TABLE 1

SUMMARY OF PROPERTIES OF COMMON BEARING MATERIALS

Material	Brinell Hardness	Minimum Shaft Hardness	Load Capacity	Max. Op. Temp.	Compat-ability	Conform-ability	Corrosion Resistance Fatigue Strength
Tin-base Babbitt	20-30	150	800-1500	300	1	1	1,5
Lead-base Babbitt	15-20	150	800-1200	300	1	1	3,5
3 layer composite Babbitt	---	230	2000-4000	225-300	1	2	2,3
Hardened Lead	22-26	225	1200-1500	500	2	2	5,5
Cadmium Base	30-40	225	1500-2000	500	1	2	5,4
Tin Bronze	60-80	350	4000	500	3	5	2,3
Lead Bronze	40-80	300	300-4500	450-500	3	4	4,2
Phosphor Bronze	75-100	400	4000	500	3	5	3,1
Aluminum Alloy	45-50	300	4000	225-300	5	3	1,2
Silver (O.P.)	25-	300	4000	500	2	3	1,1
Copper Lead	20-30	300	1500-2500	350	2	2	5,3

TABLE 2

AVERAGED COMPATIBILITY DATA FOR TIN AND LEAD BASE BABBITTS*

Material	Lubrication	Load (psi)	# Tests	Wear Rate	Max. Temp.	μ	Dwell Time
Tin Babbitt	none	340	4	.042	351	.34	0
89Sn, 7.5SB, 3.5Cu	1 drop oil	250	3	.029	262	.36	49
Tin Babbitt	none	340	2	.080	396	.28	0
83.3Sn, 8.3Sb, 8.3Cu	1 drop	250	3	.031	277	.27	35
Lead Babbitt	none	340	3	1.673	320	.34	0
76.5Pb, 15Sb, 0.5Cu, 7.5Sn, 0.5As	1 drop	250	3	.001	149	.17	10

*Run against unhardened SAE 4140 shaft steel ground to 8-16 rms microinches.

TABLE 3

AVERAGED COMPATIBILITY DATA FOR BRONZES*

Alloy	Dry Wear Rate	Dry μ	Oiled Dwell Min.
Tin Bronze	.067	.36	3
Lead Bronze	.102	.22	8
Zinc Bronze	.010	.44	151

*250 psi load 700 ft/min. surface speed, 4140 shaft steel with F3 finish.

TABLE 4

COMPATIBILITY DATA FOR ALUMINUM ALLOYS*

Alloy	Wear rate	μ	Dwell Min.
87.8Al, .8Si	.03	.25	2
3.5Fe	8.2**	.45**	1**
95Al, 4Si, 1Cd	.09	.30	1**
91.5Al, 6.5Sn, 1Ni, 1Cu	.30	.33	3

*Unhardened 4140 shaft steel; F3 finish, 250 psi load 700 ft/min. surface speed; lubricated with 1 drop oil.

**Run dry at 340 psi.

TABLE 5

COMPATIBILITY DATA FOR CARBON GRAPHITES*

Material	Wear rate (in/hr.)	μ
Best	.0002	.10
Poorest	.029	.61
Mean	.0015	.21

*Unhardened 4140 shaft steel; F3 finish; 250 psi load, 700 ft/min. surface speed.

TABLE 6

COMPATIBILITY DATA FOR PLASTICS

Material	Dry wear rate (in./hr.)	Dry μ	Oiled Dwell Min.
Nylon	1.0	.86	190-1125
Nylon = Graphite	10.0	.64	26
Teflon	.37	.17	0
Teflon + Fiberglass	.003	.30	27
Textolite 2001	.0007	.18	45
Textolite 1835	.008	.21	0
Textolite 1841A	.30	.47	55